Symmetry adapted cluster-configuration interaction study on the excited and ionized states of $TiBr_4$ and TiI_4

Hiroshi Nakatsuji and Masahiro Ehara
Department of Synthetic Chemistry and Biological Chemistry, Faculty of Engineering, Kyoto University, Kyoto 606, Japan and Institute for Fundamental Chemistry, 34-4, Takano-Nishihiraki-cho, Sakyou-ku, Kyoto 606, Japan

(Received 25 March 1994; accepted 22 July 1994)

The symmetry adapted cluster-configuration interaction (SAC-CI) method is briefly reviewed and applied to the excitation and ionization spectra of TiX_4 (X=Br, I). The valence excited states of these molecules are investigated systematically and compared with the previous study on $TiCl_4$. The experimental spectra are well reproduced and assigned by the SAC-CI calculation including spin–orbit interaction of the ligand p atomic orbital (AO) and Ti d AO. Nine A_1, ten A_2, 20 E, and 30 T_1 and T_2 states are calculated for the excited states, and the oscillator strengths are distributed among the transitions to 30 T_2 states, which cause the excitation spectra to be very complicated, especially for the TiI_4 molecule. The ordering of the ionized states in the outer valence region is $(1t_1)^{-1}<(3t_2)^{-1}<(1e)^{-1}<(2t_2)^{-1}<(2a_1)^{-1}$, which is the same as that of $TiCl_4$. The spin–orbit splittings in the $^2T_2$ states of $TiBr_4$ and TiI_4 are estimated to be smaller than those of the previous studies, and we propose a new assignment for the experimental photoelectron (PE) spectra.

I. INTRODUCTION

Titanium tetrahalides[1-6] are representative molecules of the transition metal complexes in tetrahedral coordination. Their electronic structure[1-6] and stereochemistry[7] were studied extensively by various experimental and theoretical techniques. However, there still remain some uncertainties even in the assignments of the electronic spectra of these molecules.[1-6]

In the preceding paper,[5] we have investigated the excited and ionized states of $TiCl_4$ molecule. We reproduced its excitation spectrum just below the ionization threshold and proposed detailed assignments and pictures of the excited states. We also could reproduce the ionization spectrum both in outer and inner valence regions. It is worthwhile to investigate the changes in the electronic structure caused by a systematic substitution of the ligands. Theoretical description of the electronic structures of TiX_4 (X=Br, I) is more difficult than that of $TiCl_4$ in the following two points: (1) there are five electronic valence shells in a very narrow energy region; (2) the spin–orbit effect of the ligands is large.

The experimental excitation spectrum of $TiBr_4$ in the vapor phase and that of TiI_4 in cyclohexane solution were reported.[2] These spectra are observed only for the region of the valence excitations and not for that of the Rydberg excitations. As the ligands become soft, the peaks in the experimental spectra shift toward lower energy and the spectra show more complicated structures. These trends are supposed to be caused by the lower ionization potentials and larger spin–orbit interaction of the ligands. However, there are no theoretical works which explain quantitatively these features of the spectra.

Ionization spectra of these species are systematically studied experimentally by the gas phase photoelectron spectroscopy.[3,4] Experimental spectra are assigned with the aids of the extend Hückel molecular orbital (MO) calculations. The difference in the cross section between He(I) and He(II) excitations also gives significant information about the orbital nature.[3] However, more reliable theoretical treatments including electron correlations are necessary for the systematic assignment of the spectra of these molecules.

In this paper, we theoretically investigate the excited and ionized states of TiX_4 (X=Br, I) using the symmetry adapted cluster (SAC) expansion[8] and SAC-configuration interaction (SAC-CI)[8,9] theories. The SAC/SAC-CI method describes electron correlations effectively and has been confirmed to be accurate and useful for studying spectroscopies of various excited and ionized systems.[5,10-14] The experimental spectra were well reproduced and reliable new assignments were proposed. A review article was published in Ref. 10.

We also study the spin–orbit effect of the ligands using the CI scheme and therefore, beforehand, precise descriptions of both singlet and triplet excited states are very important. The SAC-CI method, which is applicable to various spin multiplicity,[15] is suitable for the present purpose.

II. SAC/SAC-CI METHOD

The SAC wave function for the singlet ground state is written as[8]

$$\Psi_g^{\mathrm{SAC}} = e^S|0\rangle \tag{1}$$

with $S = \Sigma_I C_I S_I^\dagger$, where the excitation operator $S_I^\dagger$ should be spin-symmetry adapted, since otherwise the wave function represents a mixed symmetry, just like unrestricted Hartree–Fock (UHF) (see Thouless' theorem[16]). Detailed discussions for general open-shell systems were given in Ref. 8.

When we apply the SAC method to the ground state, we get the SAC wave function itself, and at the same time, the functions $\{\Phi_K\}$,

$$\Phi_K = PR_K^\dagger \Psi_g^{\mathrm{SAC}}, \tag{2}$$

which satisfy

 0021-9606/94/101(9)/7658/14/$6.00

$$\langle \Phi_K | \Psi_g^{SAC} \rangle = 0, \quad \langle \Phi_K | H | \Psi_g^{SAC} \rangle = 0. \tag{3}$$

In Eq. (2), P is a projector $N_g - |\Psi_g^{SAC}\rangle\langle\Psi_g^{SAC}|$, N_g being a norm of Ψ_g^{SAC}, and $R_K^\dagger$ represents a symmetry adapted excitation operator. Equation (3) means that the set of functions $\{\Phi_K\}$ spans the space for excited states. We then expand the excited state Ψ_e by a linear combination of Φ_K as

$$\Psi_e^{SAC\text{-}CI} = \sum_K d_K \Phi_K, \tag{4}$$

which is the SAC-CI method proposed in 1978.[9] The SAC-CI wave functions satisfy correct relations among ground and excited states; i.e., orthogonality and H orthogonality.[9] When we take the ionization or the electron attachment operator for $R_K^\dagger$, the SAC-CI method describes the ionized or electron-attached state, respectively. The SAC-CI wave function is also written as

$$\Psi_e^{SAC\text{-}CI} = R\Psi_g^{SAC}, \tag{5}$$

where the excitation operator R is written as $R = \Sigma_K d_K' R_K^\dagger$.

The SAC-CI theory may be formulated in a different way.[17] In an exact limit, it is easy to derive an equation-of-motion type formula

$$[H,R]\Psi_g^{SAC} = \Delta E\, R\Psi_g^{SAC}, \tag{6}$$

where ΔE is the excitation energy, $\Delta E = E_e^{SAC\text{-}CI} - E_g^{SAC}$, and R is the excitation operator in Eq. (5). From Eq. (6), we further obtain

$$\langle 0 | R_K e^{-S} [H,R] e^{S} | 0 \rangle = \Delta E \langle 0 | R_K R | 0 \rangle. \tag{7}$$

For more details, see Hirao.[17]

Both SAC and SAC-CI theories are exact, but, in actual applications, we have to introduce some approximations. We use the nonvariational solution rather than the variational one. Both procedures were discussed in detail in Ref. 9. When the nonvariational procedure is used, we have to diagonalize large nonsymmetric matrices. Since there was no such method in the literature, we had proposed a method for large nonsymmetric eigenvalue problems.[18] We approximate the levels of the excitation operators $S_I^\dagger$ and $R_K^\dagger$ to be practically accurate—up to singles and doubles for ground and one-electron excited states,[12] and up to triple and even higher for two- and many-electron processes.[19] Our SAC-CI programs can deal with singlet to septet states and can include up to eight electron excitations for $R_K^\dagger$.[20,21] The program SAC85 deals with ground, excited (singlet and triplet), cation (doublet), and anion (doublet) states with $S_I^\dagger$ and $R_K^\dagger$ operators being singles and doubles.[12,20]

The SAC/SAC-CI method has been applied to various chemically interesting phenomena involving ground, excited, and ionized states of molecules and radicals.[22] We have studied the spectroscopies of valence and Rydberg excitations and ionizations of various molecules and radicals, from Be and H_2O (Refs. 9 and 23) to benzene,[24] naphthalene,[25] and metal complexes;[26] hyperfine splitting constants of various doublet and triplet radicals;[27] potential curves and dynamics involving excited states;[28] and catalytic and surface photochemical processes.[29] Through these applications, the SAC/SAC-CI method has been well established as a simple and accurate method useful for studying chemistry and physics of molecular phenomena involving different electronic states. A review was published in Ref. 10.

Recently, a method with a slight modification from SAC-CI was published with the name of equation of motion coupled cluster (EOM-CC).[30] It uses in Eq. (5) the coupled cluster (CC) wave function (CCSD) instead of the SAC wave function and expanded the excitation operator R by single and double excitation operators. For closed shells, the SAC wave function becomes essentially the same as the CC wave function, so that the EOM-CC is the same as the SAC-CI. The difference is only minor: different approximations were adopted in practical calculations. The SAC/SAC-CI method has now already been well established, due to our pioneering efforts, not only as a theory for ground, excited, ionized, and electron-attached states, but also as a useful computational method for studying chemistry involving these different electronic states. It is therefore rather confusing to use the term EOM-CC, since it is not new, but merely an approximation of the SAC-CI method.

We further note that the coupled cluster linear response (CCLR) method due originally to Mukherjee *et al.*[31] and recently investigated by Koch *et al.*[32] is also closely related to the SAC-CI method. Actually, Eq. (7) derived above is the same as their CCLR eigenvalues equation.[33] Therefore, these two methods should be identical, at least in an exact limit, though different insights may be obtained from different formulations.

III. COMPUTATIONAL DETAILS

The geometries of TiX_4 (X=Br, I) are fixed to regular tetrahedron with the experimental bond lengths of 2.339 and 2.546 Å for $TiBr_4$ and TiI_4, respectively.[7(a)] Geometrical relaxation effects are not considered in the present study; we calculate only vertical excitations and ionizations of these molecules.

For the Ti atom, we use the same Gaussian basis set as in the previous study[5]—the $(14s8p5d)/[6s2p3d]$ set[34] augmented with two p type functions of $\zeta_p = 0.15$ and 0.073. The relativistic effective core potential (RECP) and the $(3s3p)/[2s2p]$ sets[35] are used for bromine and iodine atoms. Since we need the spectra only in the valence region, neither Rydberg type functions nor anion type functions are added on the ligands. The final basis sets for TiX_4 (X=Br, I) molecules consist of 68 CGTOs. As the reference orbitals, we use the Hartree–Fock self-consistent field (HFSCF) MOs of the ground state for all the calculations. They are calculated by the program GAMESS.[36] The numbers of the occupied and unoccupied orbitals are 25 and 43, respectively.

Electron correlations in the ground state are taken into account by the SAC theory[8] and those in the excited states by the SAC-CI theory.[9] The SAC/SAC-CI calculations are carried out by the SAC85 program.[20] Twelve higher occupied orbitals and all 43 unoccupied orbitals are used for the active space in the calculations of singlet and triplet states (active space I). For the ionized states, the active space is enlarged for the occupied space as 16 higher occupied orbitals (active space II), since we need the spectral information of the inner

TABLE I. Dimensions of the SAC/SAC-CI calculations for $TiBr_4$ and TiI_4.

State symmetry		Dimension	
T_d	C_{2v}	$TiBr_4$	TiI_4
Ground state $^1A_1$	$^1A_1$	1749	1495
Singlet excited states			
$^1T_2$, ^1E, $^1A_1$	$^1A_1$	5383	4634
$^1T_1$, ^1E, $^1A_2$	$^1A_2$	4377	4555
$^1T_1$, $^1T_2$	$^1B_1$	5402	4715
Triplet excited states			
$^3T_2$, ^3E, $^3A_1$	$^3A_1$	7189	7828
$^3T_1$, ^3E, $^3A_2$	$^3A_2$	7138	7779
$^3T_1$, $^3T_2$	$^3B_1$	7464	8108
Ground state $^1A_1$	$^1A_1$	2109	1835
Ionized states			
$^2T_2$, ^2E, $^2A_1$	$^2A_1$	1760	1714
$^2T_1$, ^2E, $^2A_2$	$^2A_2$	841	825
$^2T_1$, $^2T_2$	$^2B_1$	1531	1464

valence region. We adopt all the singly excited configurations and selected doubly excited ones for the linked terms. The contributions of the triple and quadruple excitations are taken into account by the unlinked terms. The calculations are done in the C_{2v} subset of the T_d point group. Table I gives the correspondence of the irreducible representations of C_{2v} and T_d.

Configuration selection is performed in the perturbative way[12] in order to reduce the size of the calculations. For singlet and triplet states, the thresholds λ_g and λ_e are set to 3×10^{-5} and 4×10^{-5} a.u., respectively. Reference configurations are selected from the lower 16, 14, and 15 SE-CI solutions for the A_1, A_2, and B_1 symmetries, respectively. For the ionized states, λ_g and λ_e are set to 3×10^{-5} and 1×10^{-5} a.u. The resultant dimensions of the present calculations are summarized in Table I.

The effect of spin–orbit interactions is considered for the excited and ionized states. The method has been reported previously[37] and some accounts are given in Appendix A.

IV. GROUND STATE

The HF configuration of the ground state of TiX_4 (X = Br, I) and its orbital characters are as follows: the numbering of the orbitals is due to the experimental works for the ionized states.[3,4]

Valence occupied MOs

$(1a_1)^2$ L(s) (nonbonding),

$(1t_2)^6$ L(s) (nonbonding),

$(2a_1)^2$ Ti(s)−L($p\sigma$) [Ti(s), weakly antibonding],

$(2t_2)^6$ Ti($d\sigma$)+L($p\sigma$) (σ bonding),

$(1e)^4$ Ti($d\pi$)+L($p\pi$) (π bonding),

$(3t_2)^6$ L($p\pi$) (nonbonding),

$(1t_1)^6$ L($p\pi$) (nonbonding).

Low-lying unoccupied MOs

$(2e)$ Ti($d\pi$)−L($p\pi$) (π antibonding),

$(4t_2)$ Ti(d)−L($p\sigma$,$p\pi$) (σ,π antibonding),

where Ti(x) and L(y) denote the titanium valence x orbital and ligand (Br or I) y orbital, respectively. Plus and minus signs indicate bonding and antibonding combinations, respectively. The directions of σ and π are due to those defined by Ballhausen *et al.*[38] The lowest four orbitals $1a_1$ and $1t_2$ represent s lone pair orbitals of four ligands. The next $2a_1$ orbital is Ti(s) and has a weak antibonding character. The $2t_2$ and $1e$ MOs are characterized as the bonding MOs between Ti and halogens. The highest six occupied MOs $3t_2$ and $1t_1$ are nonbonding π orbitals of the ligands. Valence occupied MOs from $2a_1$ to $1t_1$ are dominated by the ligand p atomic orbitals (AOs). The lowest unoccupied orbitals $2e$ and $4t_2$ are the antibonding MOs between Ti and the ligands and are dominated by the d AOs of Ti.

The HF energies are calculated to be −900.106 65 and −892.991 43 a.u. for $TiBr_4$ and TiI_4, respectively. The correlation energy of the ground state for $TiBr_4$ is calculated to be −0.168 52 a.u. with the active space I, while it is −0.187 19 a.u. with the active space II. Inclusion of the $(1a_1)$ and $(1t_2)$ MOs into active space improves the ground state energy by 0.018 67 a.u. for $TiBr_4$. Similarly, the correlation energy for the ground state of TiI_4 is −0.164 37 a.u. with the active space I, and −0.180 03 a.u. with the active space II.

The atomic net charges on the ligands are −0.052 ($TiBr_4$) and +0.039 (TiI_4) in the HF level using the Mulliken population analysis. Comparative value[5] for $TiCl_4$ is −0.138 for the atomic net charge on chlorine. The ionicity of the M–L bond reduces as the ligand becomes soft, as expected. We note that the Mulliken population itself is strongly basis-set dependent. The electronic part of the second moment, which indicates the size of the molecule, is 240 a.u. for $TiBr_4$ and 291 a.u. for TiI_4.

V. EXCITED STATES

All the excited states calculated in this paper are valence excitations which are characterized as the excitations from either the L lone-pair MO or the M–L bonding MO to the M–L antibonding MO. Rydberg excitations are expected to lie above 7.4 eV for $TiBr_4$ from the consideration on the term value,[1] so that the observed excitation spectrum[2] is explained within the valence excitations. This corresponds to region I in the study of $TiCl_4$.[5] For $TiBr_4$ and TiI_4, we study only the valence excitations and the Rydberg excitations are not examined here.

The valence excited states are characterized by the products of the symmetry designations of the 12 occupied MOs and the five lowest virtual MOs. For example, the excitation $2t_2\rightarrow4t_2$ gives A_1, E, T_1, and T_2 states. In this way, singly excited configurations within the 12×5 space give three A_1, two A_2, five E, seven T_1, and eight T_2 states. The present calculation deals with all of these states except for the $3\,^1A_1$ state, since it lies in higher energy region.[5,39] Among these excited states, only the transitions to the T_2 states are optically allowed in the T_d point group, and eight such $^1T_2$ states exist in the present system, though only four prominent peaks are observed in the region of the valence excitation of $TiCl_4$.

TABLE II. Excitation energy and oscillator strength for the singlet excited state of $TiBr_4$ calculated by the SAC-CI method without including spin–orbit interaction (in electron volts).

State	Dominant configurations	Excitation character	SAC-CI	
			Excitation energy	Oscillator strength
$1\,^1T_1$	$0.89(1t_1\rightarrow 2e)$	$L\rightarrow M-L$	3.20	Forbidden
$1\,^1T_2$	$0.85(1t_1\rightarrow 2e)$	$L\rightarrow M-L$	3.43	5.69×10^{-2}
$1\,^1E$	$0.89(1t_1\rightarrow 4t_2)$	$L\rightarrow M-L$	3.74	Forbidden
$2\,^1T_1$	$0.80(1t_1\rightarrow 4t_2)$, $0.08(3t_2\rightarrow 2e)$	$L\rightarrow M-L$	3.79	Forbidden
$1\,^1A_2$	$0.85(1t_1\rightarrow 4t_2)$, $0.04(1e\rightarrow 2e)$	$L\rightarrow M-L$, $M+L\rightarrow M-L$	3.84	Forbidden
$2\,^1T_2$	$0.84(1t_1\rightarrow 4t_2)$	$L\rightarrow M-L$	3.96	6.23×10^{-2}
$3\,^1T_1$	$0.52(3t_2\rightarrow 2e)$, $0.29(2t_2\rightarrow 2e)$, $0.04(1t_1\rightarrow 4t_2)$	$L\rightarrow M-L$, $M+L\rightarrow M-L$	4.32	Forbidden
$3\,^1T_2$	$0.72(3t_2\rightarrow 2e)$, $0.09(2t_2\rightarrow 4t_2)$, $0.08(2t_2\rightarrow 2e)$	$L\rightarrow M-L$, $M+L\rightarrow M-L$	4.53	6.15×10^{-2}
$2\,^1E$	$0.65(1e\rightarrow 2e)$, $0.14(3t_2\rightarrow 4t_2)$	$M+L\rightarrow M-L$, $L\rightarrow M-L$	4.60	Forbidden
$4\,^1T_1$	$0.51(2t_2\rightarrow 2e)$, $0.24(3t_2\rightarrow 2e)$, $0.05(2t_2\rightarrow 4t_2)$	$M+L\rightarrow M-L$, $L\rightarrow M-L$	4.67	Forbidden
$2\,^1A_2$	$0.85(1e\rightarrow 2e)$	$M+L\rightarrow M-L$	4.73	Forbidden
$4\,^1T_2$	$0.67(2t_2\rightarrow 2e)$, $0.11(3t_2\rightarrow 4t_2)$, $0.09(3t_2\rightarrow 2e)$	$M+L\rightarrow M-L$, $L\rightarrow M-L$	4.75	7.99×10^{-3}
$1\,^1A_1$	$0.67(1e\rightarrow 2e)$, $0.25(2t_2\rightarrow 4t_2)$	$M+L\rightarrow M-L$	4.81	Forbidden
$5\,^1T_1$	$0.70(3t_2\rightarrow 4t_2)$, $0.09(1e\rightarrow 4t_2)$, $0.05(3t_2\rightarrow 2e)$	$L\rightarrow M-L$, $M+L\rightarrow M-L$	4.99	Forbidden
$3\,E$	$0.69(3t_2\rightarrow 4t_2)$, $0.21(1e\rightarrow 2e)$,	$L\rightarrow M-L$, $M+L\rightarrow M-L$	5.17	Forbidden
$5\,^1T_2$	$0.50(3t_2\rightarrow 4t_2)$, $0.17(1e\rightarrow 4t_2)$, $0.13(2t_2\rightarrow 2e)$, $0.09(2t_2\rightarrow 4t_2)$	$L\rightarrow M-L$, $M+L\rightarrow M-L$	5.21	5.86×10^{-3}
$2\,^1A_1$	$0.76(3t_2\rightarrow 4t_2)$, $0.13(2t_2\rightarrow 4t_2)$	$L\rightarrow M-L$, $M+L\rightarrow M-L$	5.24	Forbidden
$6\,^1T_1$	$0.76(1e\rightarrow 4t_2)$, $0.11(3t_2\rightarrow 4t_2)$	$M+L\rightarrow M-L$, $L\rightarrow M-L$	5.26	Forbidden
$6\,^1T_2$	$0.54(1e\rightarrow 4t_2)$, $0.26(3t_2\rightarrow 4t_2)$, $0.05(3t_2\rightarrow 2e)$	$M+L\rightarrow M-L$, $L\rightarrow M-L$	5.34	5.93×10^{-3}
$4\,^1E$	$0.49(2a_1\rightarrow 2e)$, $0.41(2t_2\rightarrow 4t_2)$	$M+L\rightarrow M-L$	5.46	Forbidden
$7\,^1T_1$	$0.81(2t_2\rightarrow 4t_2)$, $0.06(2t_2\rightarrow 2e)$	$M+L\rightarrow M-L$	5.56	Forbidden
$5\,^1E$	$0.48(2t_2\rightarrow 4t_2)$, $0.43(2a_1\rightarrow 2e)$	$M+L\rightarrow M-L$	5.82	Forbidden
$7\,^1T_2$	$0.49(2t_2\rightarrow 4t_2)$, $0.20(2a_1\rightarrow 4t_2)$, $0.14(1e\rightarrow 4t_2)$, $0.05(2t_2\rightarrow 2e)$	$M+L\rightarrow M-L$	5.99	0.183
$8\,^1T_2$	$0.69(2a_1\rightarrow 4t_2)$, $0.10(2t_2\rightarrow 4t_2)$	$M+L\rightarrow M-L$	6.66	1.040

Assignments of the excitation spectra for $TiBr_4$ and TiI_4 are very complicated because of the existence of dense states in the valence region and the strong spin–orbit interactions and, therefore, alternative possibilities may exist in some points. Our assignments are systematically performed, referring to that for $TiCl_4$ (Ref. 5) and consistent with the ionization potentials of TiX_4 species. Detailed explanations of these assignments are given in Sec. IV E.

A. Excited states of $TiBr_4$ without including spin–orbit interaction

The excitation energies and oscillator strengths of the singlet excited states of $TiBr_4$ are summarized in Table II. The theoretically calculated spectrum is compared in Fig. 1 with the experimental absorption spectrum observed in the gas phase.[2] The excitation energies and natures of the triplet excited states are given in Table III.

The excitation spectrum of $TiBr_4$ is very similar to that of $TiCl_4$. The observed spectrum consists of three main bands. The third band has an asymmetric shape, which indicates that this band is composed of more than two peaks. These peaks are different by 0.8–1.1 eV toward the lower energy side from those of $TiCl_4$. This monotonic shift of the excitation energy is explained by the change in the ionization potential (I.P.). Furthermore, there exists a close parallel between the change in I.P. of TiX_4 for different X atoms and the change of I.P. for different halogen atoms. This is because the valence MOs are dominated by the ligand p AOs. Green *et al.*[4] also noted this tendency for the I.P.'s of the carbon tetrahalides. These relationships are shown in energy diagram in Sec. VI E.

Inclusion of the spin–orbit interaction is important for a detailed assignment and analysis of the excitation spectrum and, therefore, we briefly summarize here the natures of the singlet and triplet excited states.

First the singlet excited states of $TiBr_4$ are examined. Table II shows that the lower energy side of the spectrum is characterized as L→M−L, while the higher energy side is characterized as M+L→M−L. Among the dipole allowed $^1T_2$ states, five states have relatively large oscillator strengths. Many dipole forbidden states $^1A_1$, $^1A_2$, ^1E, and $^1T_1$ exist in the valence region. The dipole forbidden $1\,^1T_1$ state ($1t_1\rightarrow 2e$) is calculated at the lowest energy 3.20 eV of the singlet excited states. This was also observed for other transition metal complexes,[5,14] and the $^1T_1$ states are calculated to be more stable than the corresponding $^1T_2$ states by 0.08–0.43 eV. The electronic parts of the second moments of all the singlet excited states lie within 240–242 a.u. and are

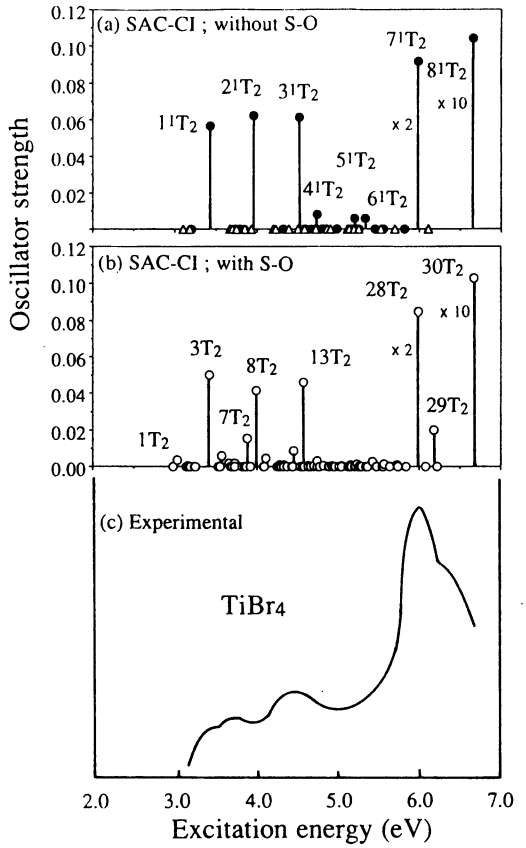

FIG. 1. Theoretical excitation spectrum of $TiBr_4$ (a) without the spin–orbit interaction [singlet (●) and triplet (△) states]; (b) including the spin–orbit interaction; and (c) experimental excitation spectrum (Ref. 2).

almost the same as that of the ground state: all of these states are valence excited states.

We next examine triplet excited states of $TiBr_4$ given in Table III. Triplet T_2 states are found to be more stable by 0.22–0.73 eV than the corresponding singlet T_2 states. The singlet–triplet separation for the T_2 symmetry is relatively large compared to those for the other symmetries; those for T_1, E, and A_2 symmetries are -0.02–-0.09, -0.07–-0.30, and $+0.01$–0.00 eV, respectively. All the $^3T_2$ states are calculated to be more stable than the corresponding $^3T_1$ states by 0.08–0.27 eV, which is the reverse to that observed for the singlet state. Triplet excited states do not necessarily have the same excitation nature as the corresponding singlet excited states. For example, the $6\,^1T_2$ state is characterized as $1e\rightarrow 4t_2$, $3t_2\rightarrow 4t_2$, and $3t_2\rightarrow 2e$, while the $6\,^3T_2$ state is characterized as $2t_2\rightarrow 4t_2$ and $3t_2\rightarrow 4t_2$.

B. Spin–orbit interaction in T_d symmetry

In the T_d point group, triplet spin transforms in the same way as the basis of the t_1 symmetry. Therefore, triplet states split as follows by the inclusion of the spin–orbit interaction:

$$^3A_1\rightarrow T_1,\quad ^3A_2\rightarrow T_2,\quad ^3E\rightarrow T_1,T_2,$$

$$^3T_1\rightarrow A_1,E,T_1,T_2,\quad ^3T_2\rightarrow A_2,E,T_1,T_2,$$

where the irreducible representations[5] on the right-hand side denote the symmetry of the spin functions. Dipole allowed T_2 states are generated from the $^3A_2$, ^3E, $^3T_1$, and $^3T_2$ states and have certain oscillator strength through the interaction with the $^1T_2$ states. In the present calculation, the spin–orbit interactions among all the valence excited states except for the $3\,^1A_1$ state are considered. Therefore, nine A_1 ten A_2, 20 E, and 30 T_1 and T_2 states are calculated. The excited states in the next higher energy region are supposed to be Rydberg excitations, as shown in the previous study,[5] so that the inclusion of these states into the spin–orbit interactions will have a small influence on the present results. The method of including the spin–orbit interaction is summarized in Appendix A.

It is useful to get the approximate spin–orbit splittings by estimating the spin–orbit interaction in a stepwise manner. For example, the $^3T_2$ state split into the A_2, three hold T_2, and five hold (T_1+E) levels under the first-order perturbation. The splitting between the A_2 and (T_1+E) levels of the lowest excited $^3T_2$ state is calculated as 0.10 and 0.20 eV for $TiBr_4$ and TiI_4, respectively.

C. Excited states of $TiBr_4$ including the spin–orbit interaction

Here, we give the assignments of the excitation spectrum of $TiBr_4$ based on the results calculated including the spin–orbit effect. There are many triplet states in the lower energy region of the spectrum as summarized in Table III. Therefore, the oscillator strengths of the $^1T_2$ states are distributed to several states through the spin–orbit interaction. Figure 1(b) shows the results including the spin–orbit interaction on the basis of the SAC/SAC-CI calculations. Table IV gives the weight of the singlet and triplet components for the T_2 states which have relatively large oscillator strengths. Some T_1 states lower in energy are also shown. Two different assignments are possible for the first and second bands, which are shown in Table IV. One assignment is due to the comparison with the excitation spectrum of $TiCl_4$ and the other is due to the shape of the calculated spectrum.

First we present the former assignment. The first band whose main peak is observed at 3.66 eV is assigned to the transition to the $3T_2$ state calculated at 3.43 eV. This state corresponds to the $1\,^1T_2$ state ($1t_1\rightarrow 2e$) and is characterized as a charge transfer state from ligand to metal. The shoulder is observed at 3.47 eV, which is located in the lower energy side by 0.19 eV of the main peak. This shoulder is assumed to be a spin-forbidden and/or a dipole-forbidden state. The candidates for the spin-forbidden state are $1\,^3T_2$ and/or $1\,^3T_1$. The $1T_2$ and $2T_2$ states are dominated by these states, as shown in Table IV, and are calculated at 3.04 and 3.16 eV, respectively, though these states have very small oscillator strengths of 3.40×10^{-3} and 6.04×10^{-4}, respectively. On the other hand, dipole-forbidden states $2T_1$(3.20 eV) and $3T_1$(3.25 eV) are also calculated ~3.20 eV and should have a certain intensity through the static and/or dynamic Jahn–Teller distortion. Since the induced intensities for these dipole forbidden transitions are not examined here, it is difficult to specify the dominant origin of this shoulder.

TABLE III. Excitation energy for the triplet excited state of $TiBr_4$ calculated by the SAC-CI method without including spin–orbit interaction (in electron volts).

State	Dominant configurations	Excitation character	Excitation energy
$1\,^3T_2$	$0.81(1t_1\rightarrow 2e)$, $0.09(1t_1\rightarrow 4t_2)$	$L\rightarrow M-L$	3.10
$1\,^3T_1$	$0.86(1t_1\rightarrow 2e)$	$L\rightarrow M-L$	3.18
$1\,^3E$	$0.87(1t_1\rightarrow 4t_2)$	$L\rightarrow M-L$	3.67
$2\,^3T_2$	$0.66(1t_1\rightarrow 4t_2)$, $0.08(1t_1\rightarrow 2e)$, $0.07(3t_2\rightarrow 2e)$	$L\rightarrow M-L$	3.70
$2\,^3T_1$	$0.74(1t_1\rightarrow 4t_2)$, $0.14(3t_2\rightarrow 2e)$	$L\rightarrow M-L$	3.75
$1\,^3A_2$	$0.84(1t_1\rightarrow 4t_2)$, $0.05(1e\rightarrow 2e)$	$L\rightarrow M-L$, $M+L\rightarrow M-L$	3.85
$1\,^3A_1$	$0.58(1e\rightarrow 2e)$, $0.24(3t_2\rightarrow 4t_2)$	$M+L\rightarrow M-L$, $L\rightarrow M-L$	3.93
$3\,^3T_2$	$0.65(3t_2\rightarrow 2e)$, $0.12(2t_2\rightarrow 2e)$, $0.10(1e\rightarrow 4t_2)$	$L\rightarrow M-L$, $M+L\rightarrow M-L$	4.20
$3\,^3T_1$	$0.44(2t_2\rightarrow 2e)$, $0.34(3t_2\rightarrow 2e)$, $0.10(1t_1\rightarrow 4t_2)$	$M+L\rightarrow M-L$, $L\rightarrow M-L$	4.23
$2\,^3E$	$0.68(1e\rightarrow 2e)$, $0.13(3t_2\rightarrow 4t_2)$	$M+L\rightarrow M-L$, $L\rightarrow M-L$	4.39
$4\,^3T_2$	$0.69(2t_2\rightarrow 2e)$, $0.11(3t_2\rightarrow 2e)$, $0.09(2t_2\rightarrow 4t_2)$	$M+L\rightarrow M-L$, $L\rightarrow M-L$	4.51
$4\,^3T_1$	$0.36(3t_2\rightarrow 2e)$, $0.35(2t_2\rightarrow 2e)$, $0.10(2t_2\rightarrow 4t_2)$	$L\rightarrow M-L$, $M+L\rightarrow M-L$	4.59
$1\,^3A_1$	$0.64(2t_2\rightarrow 4t_2)$, $0.24(1e\rightarrow 2e)$	$M+L\rightarrow M-L$	4.72
$2\,^3A_2$	$0.84(1e\rightarrow 2e)$	$M+L\rightarrow M-L$	4.73
$5\,^3T_2$	$0.62(3t_2\rightarrow 4t_2)$, $0.19(2t_2\rightarrow 4t_2)$, $0.04(2t_2\rightarrow 2e)$	$L\rightarrow M-L$, $M+L\rightarrow M-L$	4.85
$3\,^3E$	$0.34(2t_2\rightarrow 4t_2)$, $0.30(3t_2\rightarrow 4t_2)$, $0.16(2a_1\rightarrow 2e)$, $0.12(1e\rightarrow 2e)$	$M+L\rightarrow M-L$, $L\rightarrow M-L$	4.87
$5\,^3T_1$	$0.56(3t_2\rightarrow 4t_2)$, $0.21(1e\rightarrow 4t_2)$, $0.09(3t_2\rightarrow 2e)$	$L\rightarrow M-L$, $M+L\rightarrow M-L$	4.91
$6\,^3T_2$	$0.60(2t_2\rightarrow 4t_2)$, $0.21(3t_2\rightarrow 4t_2)$	$M+L\rightarrow M-L$, $L\rightarrow M-L$	5.12
$2\,^3A_1$	$0.64(3t_2\rightarrow 4t_2)$, $0.14(2t_2\rightarrow 4t_2)$, $0.11(1e\rightarrow 2e)$	$L\rightarrow M-L$, $M+L\rightarrow M-L$	5.14
$4\,^3E$	$0.41(3t_2\rightarrow 4t_2)$, $0.25(2a_1\rightarrow 2e)$, $0.14(2t_2\rightarrow 4t_2)$, $0.04(1e\rightarrow 2e)$	$M+L\rightarrow M-L$, $L\rightarrow M-L$	5.20
$6\,^3T_1$	$0.65(1e\rightarrow 4t_2)$, $0.25(3t_2\rightarrow 4t_2)$	$M+L\rightarrow M-L$, $L\rightarrow M-L$	5.20
$7\,^3T_2$	$0.77(1e\rightarrow 4t_2)$, $0.08(3t_2\rightarrow 2e)$	$M+L\rightarrow M-L$, $L\rightarrow M-L$	5.26
$7\,^3T_1$	$0.79(2t_2\rightarrow 4t_2)$, $0.08(2t_2\rightarrow 2e)$	$M+L\rightarrow M-L$	5.53
$5\,^3E$	$0.51(2a_1\rightarrow 2e)$, $0.39(2t_2\rightarrow 4t_2)$	$M+L\rightarrow M-L$	5.70
$8\,^3T_2$	$0.86(2a_1\rightarrow 4t_2)$	$M+L\rightarrow M-L$	6.11

The second band is reported to consist of the two peaks at 4.44 and 4.59 eV by the experimental work.[2] The dipole allowed states of the $7T_2$(3.89 eV), $8T_2$(4.00 eV), $12T_2$(4.45 eV), and $13T_2$(4.58 eV) states are collectively attributed to this band by the present calculation. The $7T_2$ and $8T_2$ states originate from the $2\,^1T_2$ and $1\,^3A_2$ states whose main configuration is $1t_1\rightarrow 4t_2$ as shown in Tables II and III. The $12T_2$ and $13T_2$ states are generated through the interaction of the $3\,^1T_2$ and $4\,^3T_2$ states whose dominant configurations are $3t_2\rightarrow 2e$, $2t_2\rightarrow 4t_2$, and $2t_2\rightarrow 2e$. The oscillator strengths of the transitions to the states from $14T_2$ to $27T_2$ are calculated to be small, since these states have their origin of intensity in $4\,^1T_2$, $5\,^1T_2$, and $6\,^1T_2$ states whose intensities are very small (Table II).

The other possibility for the assignment of the first and second bands is as follows. The $7T_2$ and $8T_2$ states, which are originated from the $2\,^1T_2$ state and have larger oscillator strengths than those of $TiCl_4$, are assigned to the first band with $3T_2$ assigned to the shoulder of the first band. The $12T_2$ and $13T_2$ states are then attributed to the second band.

The third band has two peaks and the lower one has a larger intensity in the experimental spectrum. We assign these peaks from the energetic point of view. The lower peak observed at 6.01 eV is assigned to the $28T_2$ state (5.99 eV) and the higher one at 6.51 eV is assigned to the $30T_2$ state (6.67 eV). The $28T_2$ and $30T_2$ states, which have large oscillator strength, originate from the $7\,^1T_2$ and $8\,^1T_2$ states, respectively. The $7\,^1T_2$ state is expressed by a linear combination of the four dominant configurations $2t_2\rightarrow 4t_2$, $2a_1\rightarrow 4t_2$, $1e\rightarrow 4t_2$, and $2t_2\rightarrow 2e$, which indicates the configuration interaction is important for describing this state quantitatively. The present calculation shows that the $8\,^1T_2$ state has larger oscillator strength than the $7\,^1T_2$ state.

All the observed peaks are assigned to the dipole allowed T_2 states. The difference Δ between the calculated excitation energy and the energy of the observed peak is shown in parentheses in Table IV. The average discrepancy between theory and experiment for the excitation energy is 0.09 eV.

D. Excited states of TiI_4

Table V gives the calculated excitation energies and oscillator strengths for the singlet excited states of TiI_4. Results for triplet excited states are also given in Table VI. Theoretical spectra including and not including the spin–orbit interaction and the experimental absorption spectrum are com-

TABLE IV. Excitation energy and oscillator strength for the excited state of $TiBr_4$ having T_2 symmetry calculated by the SAC-CI method with spin–orbit correction (in electron volts).

State[a]	Dominant configurations[b]	Excitation energy: SAC-CI (Δ[c])	Expt.[d] (Assignment[e]) (1)	(2)	Oscillator strength
$1T_2$	$0.53(1\,^3T_1), 0.40(1\,^3T_2), 0.06(1\,^1T_2)$	3.04			3.40×10^{-3}
$2T_2$	$0.55(1\,^3T_2), 0.40(1\,^3T_1), 0.005(1\,^1T_2)$	3.16	3.47		6.04×10^{-4}
$2T_1$	$0.29(1\,^3T_1), 0.29(1\,^3T_2), 0.28(1\,^1T_1)$	3.20			Forbidden
$3T_1$	$0.50(1\,^1T_1), 0.47(1\,^3T_1)$	3.25			Forbidden
$3T_2$	$0.88(1\,^1T_2)$	3.43(−0.23)	3.66	3.47	5.03×10^{-2}
$4T_2$	$0.66(2\,^3T_2), 0.10(1\,^3E), 0.10(1\,^3A_2)$ $0.04(2\,^1T_2)$	3.57			5.65×10^{-3}
$7T_2$	$0.67(1\,^3A_2), 0.22(2\,^1T_2)$	3.89			1.53×10^{-2}
$8T_2$	$0.66(2\,^1T_2), 0.20(2\,^3T_2), 0.10(1\,^3A_2)$	4.00		3.66	4.16×10^{-2}
$12T_2$	$0.60(4\,^3T_2), 0.14(3\,^1T_2), 0.10(2\,^3A_2)$	4.45(+0.01)	4.44		8.57×10^{-3}
$13T_2$	$0.75(3\,^1T_2), 0.15(4\,^3T_2)$	4.58(−0.01)	4.59		4.59×10^{-2}
$28T_2$	$0.92(7\,^1T_2)$	5.99(−0.02)	6.01		0.170
$29T_2$	$0.92(8\,^3T_2), 0.06(7\,^1T_2)$	6.18			2.00×10^{-2}
$30T_2$	$0.99(8\,^1T_2)$	6.67(+0.18)	6.51		1.029
Average discrepancy		0.09			

[a]Excited states whose oscillator strength is larger than 0.005. $1T_2$, $2T_2$, $2T_1$, and $3T_1$ states are listed for the assignments of shoulder at 3.47 eV.
[b]Dominant configurations and square values of the coefficients are listed for those square values are larger than 0.1. At least, components of singlet T_2 states are listed for triplet dominant states.
[c]Deviation from experimental values.
[d]Reference 2.
[e]Two kinds of assignments are presented (see the text).

pared in Fig. 2. Table VII summarizes the dipole allowed T_2 states having certain oscillator strengths including the spin–orbit interaction.

The spin–orbit interaction is very important for the excited states of TiI_4, as clearly seen in Fig. 2, reflecting the large spin–orbit coupling constant of the iodine atom. Strong configuration mixing between singlet and triplet states occurs, especially in the lower energy region. Oscillator strengths are considerably distributed to these T_2 states as seen from Table VII. So far, the observed absorption bands are regarded to be composed of one or a few states,[2] however, this picture does not hold for TiI_4. There exist a large number of dipole allowed transitions due to a strong spin–orbit interaction, and they cooperatively contribute to the absorption bands. Therefore, we discuss the excitation spectrum of TiI_4 using the results including the spin–orbit interaction shown in Table VII. Since the spin–orbit interaction of TiI_4 is large, the assignment reflecting the term values[1] is difficult and, therefore, it is performed on the basis of the calculated excitation energies.

The first band whose maximum is observed at 2.4 eV is assigned as being due to the $1T_2$ and $2T_2$ states calculated at 2.22 and 2.38 eV, respectively. These states originate from the $1\,^3T_1$ and $1\,^3T_2$ states and have relatively large oscillator strengths (7.57×10^{-3} and 6.41×10^{-3}) through the interaction with the $1\,^1T_2$ state. Split peaks are observed at 3.1 and 3.4 eV. The first peak is assigned to be due to the $3T_2$–$7T_2$ states and the second one to the $8T_2$–$13T_2$ states. The $7T_2$ and $9T_2$ states, which give dominant contributions to these peaks, originate from the $2\,^1T_2$ state ($3t_2\rightarrow4t_2$) and have $1\,^3A_2$ and $2\,^3T_2$ components. The third band observed at 4.3 eV is due to the $14T_2$ state calculated at 3.91 eV, which corresponds to the $3\,^1T_2$ state. The $3\,^1T_2$ state is destabilized by 0.15 eV through the spin–orbit interaction, which improve the calculated values. The $27T_2$ and $28T_2$ states calculated at 5.13 and 5.21 eV are attributed to the fourth band whose peak maximum is observed at 5.0 eV. These states are generated by the interaction of the $7\,^1T_2$ and $5\,^3E$ states. The $30T_2$ state with large oscillator strength (8.06×10^{-1}) is calculated at 6.01 eV. The experimental spectrum has no information around this energy region.

Thus all of the main observed peaks are assigned to the T_2 states. There are a number of other T_2 states which have certain oscillator strengths and these T_2 states collectively contribute to the absorption bands. The assignment of the excitation spectrum of TiI_4 is meaningless if the spin–orbit interaction is not included. The average discrepancy between theory and experiment is roughly 0.2 eV.

E. A comparison of the excited states of TiX_4

Figure 3 shows the energy diagram for the TiX_4 system (X=Cl, Br, I) based on the present and previous assignments.[5] This analysis is intrinsically qualitative and is performed for the qualitative comparison of the excitation and ionization spectra of the TiX_4 system. The energy levels are due to the experimental values[2,4] and the ionization potentials[23] of Ti^+ and halogen atoms are also given. For $TiBr_4$ and TiI_4, all levels are described by the states without including the spin–orbit interaction by averaging the corre-

TABLE V. Excitation energy and oscillator strength for the singlet excited state of TiI_4 calculated by the SAC-CI method without including the spin–orbit interaction (in electron volts).

State	Dominant configurations	Excitation character	SAC-CI	
			Excitation energy	Oscillator strength
$1\,^1T_1$	$0.89(1t_1\rightarrow 2e)$	$L\rightarrow M-L$	2.53	Forbidden
$1\,^1T_2$	$0.85(1t_1\rightarrow 2e)$	$L\rightarrow M-L$	2.73	5.39×10^{-2}
$1\,^1E$	$0.89(1t_1\rightarrow 4t_2)$	$L\rightarrow M-L$	2.94	Forbidden
$2\,^1T_1$	$0.84(1t_1\rightarrow 4t_2)$, $0.05(3t_2\rightarrow 2e)$	$L\rightarrow M-L$	2.98	Forbidden
$1\,^1A_2$	$0.87(1t_1\rightarrow 4t_2)$	$L\rightarrow M-L$	3.02	Forbidden
$2\,^1T_2$	$0.83(1t_1\rightarrow 4t_2)$	$L\rightarrow M-L$	3.16	8.69×10^{-2}
$3\,^1T_1$	$0.58(3t_2\rightarrow 2e)$, $0.26(2t_2\rightarrow 2e)$,	$L\rightarrow M-L$, $M+L\rightarrow M-L$	3.53	Forbidden
$3\,^1T_2$	$0.62(3t_2\rightarrow 2e)$, $0.16(2t_2\rightarrow 2e)$, $0.12(2t_2\rightarrow 4t_2)$	$L\rightarrow M-L$, $M+L\rightarrow M-L$	3.76	5.6×10^{-2}
$2\,^1E$	$0.60(1e\rightarrow 2e)$, $0.27(3t_2\rightarrow 4t_2)$	$M+L\rightarrow M-L$, $L\rightarrow M-L$	3.83	Forbidden
$2\,^1A_2$	$0.87(1e\rightarrow 2e)$	$M+L\rightarrow M-L$	3.97	Forbidden
$4\,^1T_1$	$0.37(3t_2\rightarrow 4t_2)$, $0.26(2t_2\rightarrow 2e)$, $0.09(3t_2\rightarrow 2e)$, $0.10(2t_2\rightarrow 4t_2)$	$L\rightarrow M-L$, $M+L\rightarrow M-L$	4.00	Forbidden
$1\,^1A_1$	$0.71(1e\rightarrow 2e)$, $0.18(2t_2\rightarrow 4t_2)$	$M+L\rightarrow M-L$	4.03	Forbidden
$4\,^1T_2$	$0.39(2t_2\rightarrow 2e)$, $0.29(3t_2\rightarrow 4t_2)$, $0.19(3t_2\rightarrow 2e)$	$M+L\rightarrow M-L$, $L\rightarrow M-L$	4.06	1.19×10^{-2}
$5\,^1T_1$	$0.35(3t_2\rightarrow 4t_2)$, $0.30(2t_2\rightarrow 2e)$, $0.11(3t_2\rightarrow 2e)$, $0.09(1e\rightarrow 4t_2)$	$L\rightarrow M-L$, $M+L\rightarrow M-L$	4.20	Forbidden
$3\,^1E$	$0.62(3t_2\rightarrow 4t_2)$, $0.28(1e\rightarrow 2e)$	$L\rightarrow M-L$, $M+L\rightarrow M-L$	4.35	Forbidden
$5\,^1T_2$	$0.36(1e\rightarrow 4t_2)$, $0.25(2t_2\rightarrow 2e)$, $0.20(3t_2\rightarrow 4t_2)$, $0.09(2t_2\rightarrow 4t_2)$	$M+L\rightarrow M-L$, $L\rightarrow M-L$	4.38	2.27×10^{-3}
$6\,^1T_1$	$0.74(1e\rightarrow 4t_2)$, $0.16(3t_2\rightarrow 4t_2)$	$M+L\rightarrow M-L$, $L\rightarrow M-L$	4.39	Forbidden
$2\,^1A_1$	$0.66(3t_2\rightarrow 4t_2)$, $0.26(2t_2\rightarrow 4t_2)$	$L\rightarrow M-L$, $M+L\rightarrow M-L$	4.49	Forbidden
$6\,^1T_2$	$0.38(3t_2\rightarrow 4t_2)$, $0.37(1e\rightarrow 4t_2)$ $0.08(2t_2\rightarrow 2e)$, $0.04(3t_2\rightarrow 2e)$	$L\rightarrow M-L$, $M+L\rightarrow M-L$	4.51	1.83×10^{-3}
$7\,^1T_1$	$0.79(2t_2\rightarrow 4t_2)$, $0.07(2t_2\rightarrow 2e)$	$M+L\rightarrow M-L$	4.75	Forbidden
$4\,^1E$	$0.78(2t_2\rightarrow 4t_2)$, $0.11(2a_1\rightarrow 2e)$	$M+L\rightarrow M-L$	4.80	Forbidden
$7\,^1T_2$	$0.59(2t_2\rightarrow 4t_2)$, $0.13(1e\rightarrow 4t_2)$, $0.08(2a_1\rightarrow 4t_2)$	$M+L\rightarrow M-L$	5.16	0.377
$5\,^1E$	$0.80(2a_1\rightarrow 2e)$, $0.07(2t_2\rightarrow 4t_2)$	$M+L\rightarrow M-L$	5.21	Forbidden
$8\,^1T_2$	$0.81(2a_1\rightarrow 4t_2)$	$M+L\rightarrow M-L$	5.95	0.893

sponding states. This analysis gives a simple and useful picture of the valence excitations and the relationship between the excitation energies and I.P.'s of these molecules, though it is very crude for TiI_4 for the neglect of the spin–orbit interaction. For $TiBr_4$, we adopt here the assignment (1) given in Table IV, which was done based on the assignment for $TiCl_4$.

The term values of $(2e)$ and $(4t_2)$ are almost the same for all the TiX_4 species, since the $2e$ and $4t_2$ MOs are dominated by the Ti d AOs. Therefore, the shift of the excitation energies accompanied by the substitution of the ligands is roughly explained by the difference of the I.P.s of TiX_4 species, which is parallel to that of the I.P.s of the ligand halogens as seen in Fig. 3.

According to the present assignment, the term values of $(2e)$ and $(4t_2)$ for $TiCl_4$ are estimated as 7.4 and 6.5 eV, if we use the experimental values. The $(2e)-(4t_2)$ splitting is estimated as 0.9 eV, which is only half of that estimated by Robin.[1] He noted that the splitting value is about twice larger than that normally seen in tetrahedral species and, therefore, our assignments seem to be reliable.

Since the $1\,^1T_2$ and $2\,^1T_2$ states are characterized as $1t_1\rightarrow 2e$ and $1t_1\rightarrow 4t_2$, the energy separation between these states gives the $(2e)-(4t_2)$ separation. In the present calculation, the $(2e)-(4t_2)$ separations of TiX_4 are calculated to reduce as the ligand becomes soft; the splitting values of 0.80, 0.53, and 0.43 eV are estimated for $TiCl_4$, $TiBr_4$, and TiI_4, respectively.

VI. IONIZED STATES

Ionization spectra of TiX_4 are divided into outer and inner valence regions.[5] In the outer valence region, there are five different electronic states, namely $(1t_1)^{-1}$, $(3t_2)^{-1}$, $(1e)^{-1}$, $(2t_2)^{-1}$, and $(2a_1)^{-1}$ states. These states lie in a low energy region and do not interact much with the ionization–excitation configurations. Therefore, Koopmans' picture is valid for these states. On the other hand, $(1a_1)^{-1}$ and $(1t_2)^{-1}$ states correspond to the ionizations from the ns orbitals of the ligands and are located in the inner valence region. These states interact with many ionization–excitation configurations through final state correlations and show a breakdown of Koopmans' picture. The spectra in the inner valence regions of $TiBr_4$ and TiI_4 are calculated similarly to that of $TiCl_4$.[5] In this paper, we concentrate our discussion on the assignments of the outer valence region.

The experimental ionization spectra of TiX_4 (X=Br, I) have a complicated structure compared with that of $TiCl_4$ even in the outer valence region. This is due to the spin–orbit interaction of the ligands and the Jahn–Teller distortion. We examine the former effect, which is larger than the latter, in the present study. With the inclusion of the spin–

TABLE VI. Excitation energy for the triplet excited state of TiI_4 calculated by the SAC-CI method without including spin–orbit interaction (in electron volts).

State	Dominant configurations	Excitation character	Excitation energy
$1\,^3T_2$	$0.78(1t_1\rightarrow 2e)$, $0.12(1t_1\rightarrow 4t_2)$	$L\rightarrow M-L$	2.43
$1\,^3T_1$	$0.84(1t_1\rightarrow 2e)$	$L\rightarrow M-L$	2.51
$1\,^3E$	$0.88(1t_1\rightarrow 4t_2)$	$L\rightarrow M-L$	2.86
$2\,^3T_2$	$0.75(1t_1\rightarrow 4t_2)$, $0.11(1t_1\rightarrow 2e)$	$L\rightarrow M-L$	2.91
$2\,^3T_1$	$0.76(1t_1\rightarrow 4t_2)$, $0.09(3t_2\rightarrow 2e)$ $0.06(1t_1\rightarrow 2e)$	$L\rightarrow M-L$	2.96
$1\,^3A_2$	$0.87(1t_1\rightarrow 4t_2)$	$L\rightarrow M-L$	3.04
$1\,^3A_1$	$0.46(1e\rightarrow 2e)$, $0.34(3t_2\rightarrow 4t_2)$, $0.13(2t_2\rightarrow 4t_2)$	$M+L\rightarrow M-L$, $L\rightarrow M-L$	3.15
$3\,^3T_1$	$0.43(3t_2\rightarrow 2e)$, $0.38(2t_2\rightarrow 2e)$	$L\rightarrow M-L$, $M+L\rightarrow M-L$	3.42
$3\,^3T_2$	$0.62(3t_2\rightarrow 2e)$, $0.17(2t_2\rightarrow 2e)$, $0.10(1e\rightarrow 4t_2)$	$M+L\rightarrow M-L$, $L\rightarrow M-L$	3.43
$2\,^3E$	$0.60(1e\rightarrow 2e)$, $0.28(3t_2\rightarrow 4t_2)$	$M+L\rightarrow M-L$, $L\rightarrow M-L$	3.63
$4\,^3T_2$	$0.40(2t_2\rightarrow 2e)$, $0.20(2t_2\rightarrow 4t_2)$, $0.16(3t_2\rightarrow 4t_2)$, $0.12(3t_2\rightarrow 2e)$	$M+L\rightarrow M-L$, $L\rightarrow M-L$	3.82
$2\,^3A_1$	$0.45(2t_2\rightarrow 4t_2)$, $0.38(1e\rightarrow 2e)$	$M+L\rightarrow M-L$	3.88
$4\,^3T_1$	$0.34(3t_2\rightarrow 4t_2)$, $0.21(2t_2\rightarrow 2e)$, $0.17(3t_2\rightarrow 2e)$, $0.12(2t_2\rightarrow 4t_2)$	$L\rightarrow M-L$, $M+L\rightarrow M-L$	3.89
$2\,^3A_2$	$0.86(1e\rightarrow 2e)$	$M+L\rightarrow M-L$	3.96
$5\,^3T_2$	$0.48(3t_2\rightarrow 4t_2)$, $0.06(1e\rightarrow 4t_2)$, $0.27(2t_2\rightarrow 2e)$	$L\rightarrow M-L$, $M+L\rightarrow M-L$	3.98
$3\,^3E$	$0.36(3t_2\rightarrow 4t_2)$, $0.25(2t_2\rightarrow 4t_2)$, $0.24(1e\rightarrow 2e)$, $0.05(2a_1\rightarrow 2e)$	$L\rightarrow M-L$, $M+L\rightarrow M-L$	4.02
$5\,^3T_1$	$0.26(3t_2\rightarrow 4t_2)$, $0.21(1e\rightarrow 4t_2)$, $0.21(3t_2\rightarrow 2e)$, $0.19(2t_2\rightarrow 2e)$	$L\rightarrow M-L$, $M+L\rightarrow M-L$	4.12
$6\,^3T_1$	$0.61(1e\rightarrow 4t_2)$, $0.28(3t_2\rightarrow 4t_2)$	$M+L\rightarrow M-L$, $L\rightarrow M-L$	4.34
$6\,^3T_2$	$0.44(1e\rightarrow 4t_2)$, $0.30(2t_2\rightarrow 4t_2)$, $0.08(3t_2\rightarrow 2e)$	$M+L\rightarrow M-L$, $L\rightarrow M-L$	4.36
$3\,^3A_1$	$0.50(3t_2\rightarrow 4t_2)$, $0.34(2t_2\rightarrow 4t_2)$	$L\rightarrow M-L$, $M+L\rightarrow M-L$	4.38
$7\,^3T_2$	$0.39(2t_2\rightarrow 4t_2)$, $0.31(1e\rightarrow 4t_2)$ $0.21(3t_2\rightarrow 4t_2)$, $0.04(3t_2\rightarrow 2e)$	$M+L\rightarrow M-L$, $L\rightarrow M-L$	4.39
$4\,^3E$	$0.46(2t_2\rightarrow 4t_2)$, $0.27(3t_2\rightarrow 4t_2)$ $0.14(2a_1\rightarrow 2e)$	$M+L\rightarrow M-L$	4.51
$7\,^3T_1$	$0.77(2t_2\rightarrow 4t_2)$, $0.12(2t_2\rightarrow 2e)$	$M+L\rightarrow M-L$, $L\rightarrow M-L$	4.70
$5\,^3E$	$0.72(2a_1\rightarrow 2e)$, $0.12(2t_2\rightarrow 4t_2)$	$M+L\rightarrow M-L$	5.10
$8\,^3T_2$	$0.87(2a_1\rightarrow 4t_2)$	$M+L\rightarrow M-L$	5.48

orbit interaction, doublet ionized states in the T_d point group are transformed into the states in spinor double group T_d^* as follows:[4,41,42]

$$^2A_1\rightarrow E'(2),\quad ^2A_2\rightarrow E''(2),\quad ^2E\rightarrow U'(4),$$

$$^2T_1\rightarrow U'(4),E'(2),\quad ^2T_2\rightarrow U'(4),E''(2),$$

where the numbers in the parentheses show the degree of the degeneracy.

Theoretical outer valence ionization potentials of TiX_4 (X=Br, I) are compared with the experimental values in Tables VIII and IX. Monopole intensities and the weight of degeneracy are also given. Theoretical I.P.s are given including first and up to second order effects of spin–orbit interaction as S–O(1) and S–O(2), respectively. The present assignments of the spectra are shown schematically with the experimental spectra in Fig. 4. The calculated spin–orbit splitting values of the $^2T_1$ and $^2T_2$ states are summarized in Table X. The splitting pattern of the triply degenerated states $^2T_1$ and $^2T_2$ is as follows: the U' state is more stable than the E' and E'' states in the case of the $(1t_1)^{-1}$ and $(3t_2)^{-1}$ states because they are all hole states. However, the ordering between U' and E'' states is reversed in the $(2t_2)^{-1}$ state. Edgell *et al.* assigned their experimental photoelectron spectra of TiX_4 (X=Br, I) using extended Hückel MOs.[3] Their results are compared in these tables and Fig. 4.

A. $TiBr_4$

Here we discuss the outer valence region of $TiBr_4$. Following the notation of the experimental spectrum,[3] the bands a and b are assigned to the U' and E' states split from the $(1t_1)^{-1}$ state. The spacing between these components is calculated to be 0.238 eV, which is in good agreement with the experimental value 0.24 eV. As for band c, the relative intensity of the experimental spectrum indicates that this band is composed of four-hold states and two-hold states. The $U'(3t_2^{-1})$ and $E''(3t_2^{-1})$ components are attributed to this band in our calculation, but Edgell *et al.* assigned this band to $U'[3t_2^{-1}(\pi)]$ and $E''[2t_2^{-1}(\sigma)]$ states. Our assignment is different from theirs since our spin–orbit splitting of the $(3t_2)^{-1}$ state (0.133 eV) is smaller than theirs. The reason for this difference will be discussed later. In the same way, we propose different assignment for band d; the $U'(1e^{-1})$, $E''(2t_2^{-1})$, and $U'(2t_2^{-1})$ states are assigned to this overlapping band. The band e is attributed to the $E'(2a_1^{-1})$ state.

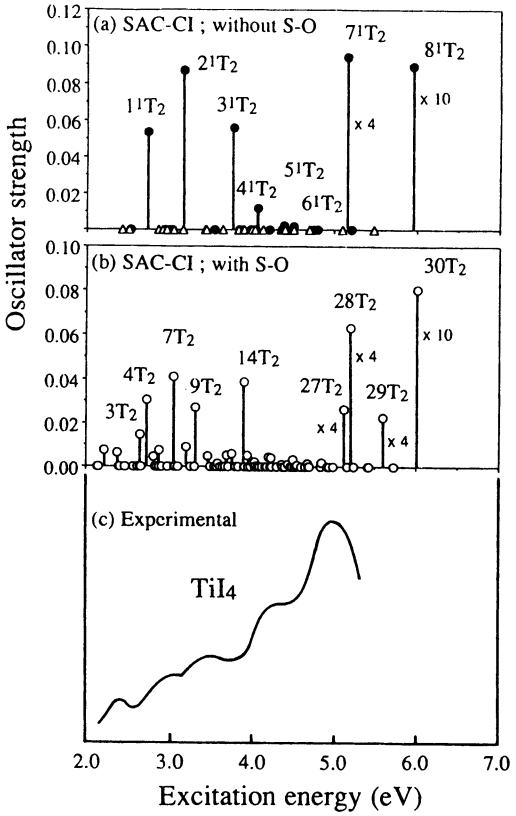

FIG. 2. Theoretical excitation spectrum of TiI_4 (a) without the spin–orbit interaction [singlet (●) and triplet (△) states]; (b) including the spin–orbit interaction; and (c) experimental excitation spectrum (Ref. 2).

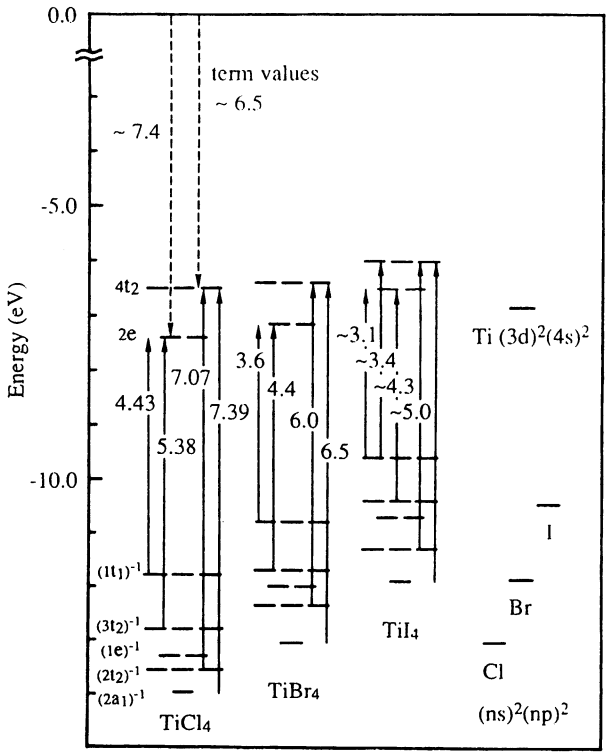

FIG. 3. An approximate schematic energy diagram of TiX_4 (X=Cl, Br, I). Assignments of the present study are shown with experimental excitation energies (in electron volts). Experimental values are cited from Ref. 2, 3, and 6(a).

Relative intensities of the bands *d* and *e* increase remarkably by changing He(I) into He(II) excitations of the experimental spectra.[3] The ionizations from the MOs having metal *s* or *d* character have larger cross sections under the He(II) excitation.[3,6(f)] Accordingly, $1e$ and $2t_2$ orbitals have metal *d* character and $2a_1$ orbital has metal *s* character.

In summary, the present assignments are different from the EHMO ones in the following two points:

(1) the ordering of the $(1e)^{-1}$ and $(2t_2)^{-1}$ states;

(2) the spin–orbit splitting of the $(3t_2)^{-1}$ and $(2t_2)^{-1}$ states.

The difference between the two assignments are clearly seen from Fig. 4 and Table VIII. As discussed in the previous paragraph, our assignments are consistent with the experimental spectra in the following points. (a) the weight of the degeneracy in our assignment explains the ratio of the band area; (b) the changes in the ionization cross section of the band under the He(II) excitation are consistent with our results; (c) the average discrepancy between theory and experiment for the ionization spectra of $TiBr_4$ is only 0.27 eV.

Next we analyze in a stepwise manner the effect of the spin–orbit interaction. We first investigate the first order effect which determines a large part of the spin–orbit splitting. It is well-known that the first order effects of the spin–orbit interaction on the T_2 and T_1 terms are similar to those on the *P* term for atoms. In this sense, Green *et al.* proposed explicit forms of the effective S–O coupling constants ζ_{eff} as[4]

$$\zeta_{t2}=C_{t2p}^2\zeta_p^M-C_{t2d}^2\zeta_d^M+\tfrac{1}{2}C'_{t2\pi}(C'_{t2\pi}-2\sqrt{2}C'_{t2\sigma})\zeta_p^L,$$

$$\zeta_{t1}=\tfrac{1}{2}(1+S_{t1\pi})^{-1}\zeta_p^L, \quad C_{t2k}=(1+S_{t2k})^{-1}C_{t2k},$$

where ζ_p^M, ζ_d^M, and ζ_p^L denote the spin–orbit coupling constants for the valence *p* and *d* orbitals of the metal atom M and the ligand L. *C* and *S* are the MO coefficient and the overlap term, respectively. Though our approach is different, the interpretation of the spin–orbit splitting is performed in terms of these useful constants.

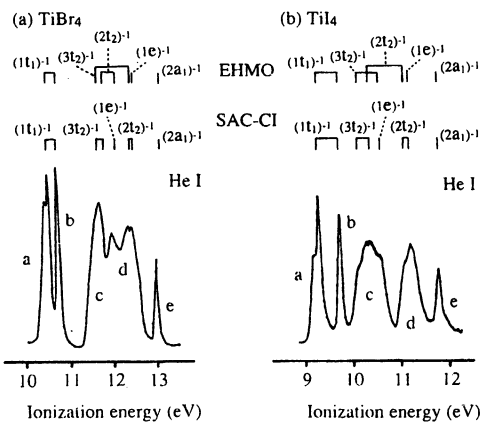

FIG. 4. Ionization spectra in the outer valence region and their theoretical assignments of (a) $TiBr_4$ and (b) TiI_4.

TABLE VII. Excitation energy and oscillator strength for the excited state of TiI_4 having T_2 symmetry calculated by the SAC-CI method including the spin–orbit correction (in electron volts).

State	Dominant configurations[b]	Excitation energy: SAC-CI (Δ)[c]	Excitation energy: Expt.[d]	Oscillator strength
$1T_2$	$0.60(1\,^3T_1)$, $0.24(1\,^3T_2)$, $0.14(1\,^1T_2)$	2.22		7.57×10^{-3}
$2T_2$	$0.42(1\,^3T_2)$, $0.14(1\,^3T_1)$, $0.11(1\,^3A_2)$ $0.10(2\,^3T_2)$, $0.04(2\,^1T_2)$	2.38(−0.05)	2.4	6.41×10^{-3}
$3T_2$	$0.29(2\,^3T_2)$, $0.21(1\,^1T_2)$, $0.20(1\,^3T_1)$ $0.11(1\,^3T_2)$, $0.10(1\,^3A_2)$	2.65		1.45×10^{-2}
$4T_2$	$0.50(1\,^1T_2)$, $0.16(1\,^3T_1)$, $0.15(2\,^3T_2)$	2.73		3.05×10^{-2}
$6T_2$	$0.74(2\,^3T_1)$, $0.04(2\,^1T_2)$, $0.03(3\,^1T_2)$	2.89	3.1	7.59×10^{-3}
$7T_2$	$0.45(2\,^1T_2)$, $0.43(1\,^3A_2)$	3.05(−0.05)		4.10×10^{-2}
$8T_2$	$0.33(3\,^3T_1)$, $0.29(3\,^3T_2)$, $0.12(3\,^1T_2)$	3.20		9.17×10^{-3}
$9T_2$	$0.29(2\,^1T_2)$, $0.28(2\,^3T_2)$, $0.21(1\,^3A_2)$	3.31(−0.09)	3.4	2.72×10^{-2}
$10T_2$	$0.42(2\,^3E)$, $0.12(4\,^3T_2)$, $0.12(4\,^3T_1)$ $0.07(4\,^1T_2)$	3.46		5.01×10^{-3}
$12T_2$	$0.41(4\,^3T_2)$, $0.26(2\,^3A_2)$ $0.08(4\,^1T_2)$	3.70		5.12×10^{-3}
$13T_2$	$0.30(3\,^3E)$, $0.24(5\,^3T_2)$, $0.15(2\,^3E)$ $0.06(3\,^1T_2)$	3.75		6.13×10^{-3}
$14T_2$	$0.69(3\,^1T_2)$	3.91(−0.39)	4.3	3.87×10^{-2}
$15T_2$	$0.24(2\,^3A_2)$, $0.18(4\,^3T_2)$, $0.17(6\,^3T_2)$ $0.11(2\,^3E)$, $0.06(4\,^1T_2)$	3.94		5.22×10^{-3}
$27T_2$	$0.67(5\,^3E)$, $0.28(7\,^1T_2)$	5.13	5.0	1.06×10^{-1}
$28T_2$	$0.66(7\,^1T_2)$, $0.27(5\,^3E)$	5.21(+0.21)		2.52×10^{-1}
$29T_2$	$0.87(8\,^3T_2)$, $0.09(8\,^1T_2)$	5.59		9.05×10^{-2}
$30T_2$	$0.90(8\,^1T_2)$	6.01		8.06×10^{-1}
Average discrepancy		0.16		

[a]Excited states whose oscillator strength is larger than 0.005.
[b]Dominant configurations and square values of the coefficients listed for those square values are larger than 0.1. At least, components of singlet T_2 states are listed for triplet dominant states.
[c]Deviation from experimental values.
[d]Reference 2.

From the above equations, ζ_{t1} may be approximated as $\frac{1}{2}\zeta_p^L$ and our calculation also reproduces t_1 splitting (0.238 eV for $TiBr_4$). This was also obtained in the previous studies.[3,4] On the other hand, our estimation of the splitting of the $(3t_2^{-1})$ state is different from the previous one as mentioned above. Edgell *et al.* calculated the splitting value fairly large for this state.[3] This is because their $3t_2$ MO is composed of both σ and π components of the ligand p AOs (see Appendix B of Ref. 4). We examine the nature of the $3t_2$ MO for the AB_4 system as shown in Appendix B and find that the $3t_2$ MO of TiX_4 (X=Br, I) has pure π components. Therefore, our estimated splitting values are relatively small compared to the previously estimated ones. However, the nature of the $3t_2$ MO is somewhat dependent on the basis set used, so that the estimation of the spin–orbit splitting for the t_2 symmetry is very delicate. In the same way, the $2t_2$ MO has pure σ-bonding nature between the metal and ligand. Therefore, the third term in the expression of the ζ_{t2} term becomes small and has a negative sign, resulting in the ordering between the E'' and U' states being reversed. The effect of d AO on the Ti atom is small since the valence MO is dominated by the ligands and the coupling constant ζ_d^M is small (0.073 eV).

We next consider the effect of the second order correction, i.e., the interaction between different irreducible representations of the T_d point group, but within the same ones in the T_d^* group. With this interaction, the $(1t_1)^{-1}$ and $(3t_2)^{-1}$ states are stabilized; while the other states are destabilized. The second-order energy perturbations of the U' states are smaller than those of the E' and E'' states. Therefore, the E' and E'' states are stabilized more than the U' state, hence the splittings of the $(1t_1)^{-1}$ and $(3t_2)^{-1}$ states become small. On the other hand, the E'' state split from the $(2t_2)^{-1}$ state is calculated as unstable compared to the U' state. Since the second order interaction works to destabilize these states, the splitting of the $(2t_2)^{-1}$ state becomes large through this interaction.

B. TiI_4

The ordering of the outer valence ionization potentials of TiI_4 is again the same as that of $TiCl_4$ (Ref. 5) as shown in Table IX and Fig. 4. Bands a and b are assigned to the U' and E' states $(1t_1^{-1})$ and the spin–orbit splitting is calculated to be 0.482 eV. The splitting of band a is due to the Jahn–Teller distortion as reported by Edgell *et al.*[3] Band c is composed of two four-hold states and one two-hold state from the consideration of the ratio of the band area, and we assign the $(3t_2)^{-1}$ and $(1e)^{-1}$ states to this band. The split band d is attributed to the $(2t_2)^{-1}$ state. The separation between U' and E'' states is also calculated to be small compared with

TABLE VIII. Outer valence ionization potential of $TiBr_4$ (in electron volts).

	Expt.[a]				SAC-CI						
			Band area								
Peak	ΔE	Assignment by EHMO	He(I)	He(II)	Assignment	ΔE[b]	ΔE [S–O(1)][c]	ΔE [S–O(2)][d]	Δ[e]	(Degeneracy)	Intensity[f]
a	10.55	$U'[t_1(\pi)]$	2.0	2.0	$U'(1t_1^{-1})$	10.13	10.050	10.039	−0.51	(4)	0.94
	10.63										
b	10.86	$E'[t_1(\pi)]$	1.0	1.3	$E'(1t_1^{-1})$		10.290	10.277	−0.57	(2)	
c	11.68	$U'[t_2(\pi)]$	2.5	3.0	$U'(3t_2^{-1})$	11.51	11.461	11.444	−0.24	(4)	0.92
		$E''[t_2(\sigma)]$			$E''(3t_2^{-1})$		11.609	11.576		(2)	
d	12.00	$U'[t_2(\sigma)]$	5.1	7.6	$U'(1e^{-1})$	11.96	11.960	11.940	−0.06	(4)	0.92
	12.31	$E''[t_2(\pi)]$			$E''(2t_2^{-1})$	12.28	12.280	12.313	+0.00	(2)	0.90
	12.42	$U'[e(\pi)]$			$U'(2t_2^{-1})$		12.281	12.328	−0.09	(4)	
	12.55(*s*)										
e	13.04	$E'[a_1(\sigma)]$	0.7	1.2	$E'(2a_1^{-1})$	12.64	12.640	12.653	−0.39	(2)	0.91
	Average discrepancy								0.27		

[a]Reference 3.
[b]Without spin–orbit correction.
[c]First order correction is included (see the text).
[d]First and second order corrections are included (see the text).
[e]Deviation from the experimental value.
[f]Monopole intensities without including the initial state correlation.

the previous studies as explained in $TiBr_4$. Band *e* is assigned to the $(2a_1)^{-1}$ state. The calculated ionization potentials underestimate the experimental values, especially for the $(1t_1)^{-1}$ and $(2a_1)^{-1}$ states. The average discrepancy between theory and experiment for the ionization potentials of TiI_4 is 0.30 eV.

VII. SUMMARY

In this paper, we briefly reviewed the SAC/SAC-CI method and applied to the study of the excited and ionized states of TiX_4(X=Br, I). The effects of the spin–orbit interactions of the ligand *p* AO and Ti *d* AO are examined both for the excited and ionized states.

The excitation spectra in the valence region are investigated and the theoretical assignments are proposed. The lowest 49 states are calculated in the valence region without including the spin–orbit interaction, namely, two A_1, two A_2, five E, seven T_1, and eight T_2 states for the singlet and triplet states. Including the spin–orbit effect, these states split into nine A_1, ten A_2, 20 E, and 30 T_1 and T_2 states. Dipole-allowed T_2 states are generated from the $^3A_2$, ^3E, $^3T_1$, and $^3T_2$ states and have certain oscillator strengths through the interaction with the $^1T_2$ states. This effect is important especially for the TiI_4 molecule. The shift of the excitation energy due to the ligand substitution is explained by the shift in the ionization potentials of these molecules, which is further attributed to the change of the ionization potentials of the ligand atoms. Theoretical results reproduce well the experimental spectra with the average discrepancies of 0.09 and 0.16 eV for $TiBr_4$ and TiI_4, respectively.

The present results also show good agreement with the experimental ionization spectra in the outer valence region. The ordering of the ionized states in the outer valence region is $(1t_1)^{-1}<(3t_2)^{-1}<(1e)^{-1}<(2t_2)^{-1}<(2a_1)^{-1}$, which is the same as that of $TiCl_4$.[5] Koopmans' picture is valid for

TABLE IX. Outer valence ionization potential of TiI_4 (in electron volts).

	Expt.[a]				SAC-CI						
			Band area								
Peak	ΔE	Assignment by EHMO	He(I)	He(II)	Assignment	ΔE[b]	ΔE [S–O(1)][c]	ΔE [S–O(2)][d]	Δ[e]	(Degeneracy)	Intensity[f]
a	9.22(*s*)	$U'[t_1(\pi)]$	2.0	2.0	$U'(1t_1^{-1})$	8.82	8.657	8.619	−0.60	(4)	0.94
	9.32										
b	9.77	$E'[t_1(\pi)]$	1.1	1.3	$E'(1t_1^{-1})$		9.145	9.102	−0.67	(2)	
c	10.23(*s*)	$E''[t_2(\sigma)]$	5.2	9.2	$U'(3t_2^{-1})$	10.24	10.113	10.064	−0.17	(4)	0.92
	10.45	$U'[t_2(\pi)]$			$E''(3t_2^{-1})$		10.494	10.363	−0.09	(2)	
	10.68	$U'[t_2(\sigma)]$			$U'(1e^{-1})$	10.56	10.560	10.490	−0.19	(4)	0.92
d	11.19(*s*)	$E''[t_2(\pi)]$	3.4	5.8	$E''(2t_2^{-1})$	10.93	10.879	11.010	−0.18	(2)	0.90
	11.34	$U'[e(\pi)]$			$U'(2t_2^{-1})$		10.956	11.111	−0.23	(4)	
e	11.92	$E'[a_1(\sigma)]$	0.9	1.7	$E'(2a_1^{-1})$	11.59	11.590	11.613	−0.30	(2)	0.91
	Average discrepancy								0.30		

[a]Reference 3.
[b]Without spin–orbit correction.
[c]First order correction is included (see the text).
[d]First and second order corrections are included (see the text).
[e]Deviation from the experimental value.
[f]Monopole intensities without including the initial state correlation.

TABLE X. Spin–orbit splitting of the $^2T_1$ and $^2T_2$ states of TiX_4 (X=Br, I) (in electron volts).

	$TiBr_4$				TiI_4		
	Expt.		Calc.			Calc.	
State	Edgell[a]	Green[b]	S–O(1)[c]	S–O(2)[d]	Expt.[b]	S–O(1)[c]	S–O(2)[d]
$(1t_1)^{-1}$	0.24	0.23, 0.25[e]	0.240	0.238	0.45, 0.54[e]	0.488	0.482
$(3t_2)^{-1}$	0.10	···	0.148	0.133	0.22	0.381	0.289
$(2t_2)^{-1}$	−0.15	−0.11	−0.001	−0.014	−0.15	−0.077	−0.102

[a]Reference 3.
[b]Reference 4.
[c]First order correction is included (see the text).
[d]First and second order corrections are included (see the text).
[e]Splitting due to vibronic coupling.

these states. The spin–orbit splitting of the peak in the present calculation explains the ratio of the band area in the experimental spectra. The change in the ionization cross section observed in the He(I) and He(II) excitation spectra is also consistent with our results. The spin–orbit splitting of the $^2T_2$ states is related to the nature of the ionized MOs. In the case of TiX_4 (X=Br, I) system, the $2t_2$ MO has pure σ-bonding nature, while the $3t_2$ MO is pure π bonding between metal and ligand. Therefore, our estimated splitting values are relatively small compared to the previous ones.[3]

ACKNOWLEDGMENTS

The calculations have been carried out with the Hitac M-680H and S-820 computers at the Institute for Molecular Science. This study has been supported by the Grant in aid for Scientific Research from the Japanese Ministry of Education, Science, and Culture.

APPENDIX A

The calculation of the spin–orbit interaction is performed using the one-electron, one-center approximation. We neglect spin–other-orbit terms and cross integrals on different centers. The expression of the spin–orbit Hamiltonian is

$$H_{IJ}=E_I\delta_{IJ}+\langle I|H^{\mathrm{so}}|J\rangle, \quad H^{\mathrm{so}}=\sum_i \sum_A \zeta(r_{iA})l_{iA}s_i,$$

where $\zeta(r_{iA})$ is the spin–orbit coupling constants of atom A, l_{iA} is the orbital angular momentum operator centered at atom A for the ith electron, and E_I is the SAC-CI energy. The matrix element $\langle I|H^{\mathrm{SO}}|J\rangle$ is calculated considering the spin–orbit interaction of the titanium d AOs and the ligand p AOs. All the symmetries of the subgroup C_{2v} are included for the state functions because of the degeneracy in the Td point group. The state functions I and J are approximated by the singly excited configuration part of the calculated excited state and by the Koopmans part for the ionized states. For valence excitations, the squares of the norms of the singly excited part in the linked terms are 0.95–0.93. The calculated monopole intensities are large (0.94–0.90) for the ionized states in the outer valence region as shown in Tables VIII and IX. These facts support the validity of the present approximation in the calculation. The spin–orbit coupling constants are estimated from the experimental spectral data;[40] those of the $3d$ AO of Ti^+, the $4p$ AO of Br, and the $5p$ AO of I are 0.011, 0.305, and 0.628 eV, respectively.

APPENDIX B

The spin–orbit splitting values for the $(2t_2)^{-1}$ and $(3t_2)^{-1}$ states of TiX_4 are estimated rather small in comparison with those in previous works.[3,4] Since the present system shows complicated splitting structure, we refer to the ionization spectra of CBr_4 and $SiBr_4$. The splitting pattern of these molecules is clear because $2a_1$ and $2t_2$ orbitals are dominated by $2s$ and $2p$ AOs of the central carbon atom. The experimental photoelectron spectra of those molecules show large splitting for the $(3t_2)^{-1}$ state (about 0.45 eV). Therefore, we examine the spin–orbit splitting of the $^2T_1$ and $^2T_2$ terms for CBr_4 and $SiBr_4$. Results are summarized in Table XI.

The splitting value of the $(3t_2)^{-1}$ state of CBr_4 is calculated as 0.451 eV in good agreement with the experimental value 0.46 eV.[4] The splitting values of CBr_4 are calculated very large compared to those of $TiBr_4$. We explain this fact in terms of the bonding natures of the ionized MO. The $2t_2$ and $3t_2$ MOs of the CBr_4 molecule are C–L bonding and ligand nonbonding MOs, respectively, such as the TiX_4 system. However, π and σ components of the ligand p AOs mix in both MOs of CBr_4. In other words, both the $2t_2$ and $3t_2$ MOs of CBr_4 still keep the degeneracies of the p AO of the bromine atom. Therefore, as seen from the expression of the effective coupling constant in the text, the splittings of the $(2t_2)^{-1}$ and $(3t_2)^{-1}$ states of CBr_4 become large. The same is true for the spin–orbit interaction of $SiBr_4$. On the other hand, the $2t_2(3t_2)$ MO of TiX_4 has pure $\sigma(\pi)$ components of the ligand AOs, therefore, the splitting of the T_2 term be-

TABLE XI. Spin–orbit splitting of the $^2T_1$ and $^2T_2$ states of ABr_4 (A=C, Si) (in electron volts).

	CBr_4		$SiBr_4$	
State	Expt.[a]	Calc.[b]	Expt.[a]	Calc.[b]
$(1t_1)^{-1}$	0.26, 0.35[c]	0.270	0.27, 0.36[c]	0.255
$(3t_2)^{-1}$	0.46, 0.64[c]	0.451	0.42, 0.53[c]	0.389
$(1t_1)^{-1}$	···	−0.091	···	−0.124

[a]Reference 4.
[b]First and second order corrections are included (see the text).
[c]Splitting due to vibronic coupling.

comes small. Thus, we see that the difference in the spin–orbit splitting between $TiBr_4$ and CBr_4 originates from the difference in their bonding characters.

[1] M. B. Robin, *Higher Excited States of Polyatomic Molecules* (Academic, New York, 1975), Vol. 2.

[2] L. DiSipio, G. DeMichelis, E. Tondello, and L. Oleari, Gazz. Chim. Ital. **96**, 1785 (1966).

[3] R. G. Egdell and A. F. Orchard, J. Chem. Soc. Faraday Trans. 2 **74**, 485 (1978).

[4] J. C. Green, M. L. H. Green, P. J. Joachim, A. F. Orchard, and D. W. Turner, Philos. Trans. R. Soc. London, Ser. A **268**, 111 (1970).

[5] H. Nakatsuji, M. Ehara, M. H. Palmer, and M. F. Guest, J. Chem. Phys. **97**, 2561 (1992).

[6] (a) C. A. Becker, C. J. Ballhausen, and I. Trabjerg, Theoret. Chim. Acta **355**, 13 (1969); (b) J. S. Tse, Chem. Phys. Lett. **373**, 15 (1981); (c) A. A. Inverson and B. R. Russell, Spectrochimica Acta Part A **29**, 715 (1973); (d) A. E. Foti, V. H. Smith, Jr., and M. A. Whitehead, Mol. Phys. **45**, 385 (1982); (e) W. von Niessen, Inorg. Chem. **26**, 567 (1987); (f) G. M. Bancroft, E. Pellach, and J. S. Tse, Inorg. Chem. **21**, 2950 (1982).

[7] (a) Y. Morino and U. Uehara, J. Chem. Phys. **45**, 4543 (1966); (b) M. F. A. Dove, J. A. Creighton, and L. A. Woodward, Spectrochim. Acta **18**, 267 (1962); (c) J. K. Wilmshurst, J. Mol. Spectrosc. **5**, 343 (1960).

[8] H. Nakatsuji and K. Hirao, Chem. Phys. Lett. **47**, 569 (1977); J. Chem. Phys. **68**, 2053 (1978).

[9] H. Nakatsuji, Chem. Phys. Lett. **59**, 362 (1978); **67**, 329 (1979); **67**, 334 (1979).

[10] H. Nakatsuji, Acta Chim. Hung. **129**, 719 (1992).

[11] H. Nakatsuji, K. Ohta, and K. Hirao, J. Chem. Phys. **75**, 2952 (1981).

[12] H. Nakatsuji, Chem. Phys. **75**, 425 (1983).

[13] H. Nakatsuji, J. Chem. Phys. **80**, 3703 (1984).

[14] H. Nakatsuji and S. Saito, J. Chem. Phys. **91**, 6205 (1989).

[15] H. Nakatsuji and M. Ehara, J. Chem. Phys. **98**, 7179 (1993).

[16] D. J. Thouless, Nucl. Phys. **21**, 225 (1960); **22**, 78 (1961).

[17] K. Hirao, J. Chem. Phys. **79**, 5000 (1983).

[18] K. Hirao and H. Nakatsuji, J. Comp. Phys. **45**, 246 (1982).

[19] H. Nakatsuji, Chem. Phys. Lett. **177**, 331 (1991).

[20] H. Nakatsuji, program system for SAC and SAC-CI calculations, Program Library No. 146 (Y4/SAC), Data Processing Center of Kyoto University, 1985; Program Library SAC85, No. 1396, Computer Center of the Institute for Molecular Science, Okazaki, 1986.

[21] H. Nakatsuji, program system for exponentially generated wave functions for ground, excited, ionized, and electron attached states.

[22] A review of the SAC/SAC-CI studies for 1977–1991 was published in Ref. 10. For more recent studies, see references of H. Nakatsuji, M. Ehara, and T. Momose, J. Chem. Phys. **100**, 5821 (1994); S. Jitsuhiro, H. Nakai, M. Hada, and H. Nakatsuji, *ibid.* **101**, 1029 (1994).

[23] H. Nakatsuji and K. Hirao, Int. J. Quantum Chem. **20**, 1301 (1981); Chem. Phys. Lett. **79**, 292 (1981); H. Nakatsuji and T. Yonezawa, *ibid.* **87**, 426 (1982).

[24] O. Kitao and H. Nakatsuji, J. Chem. Phys. **87**, 1169 (1987).

[25] H. Nakatsuji, M. Komori, and O. Kitao, Chem. Phys. Lett. **142**, 446 (1987).

[26] S. Jitsuhiro, H. Nakai, M. Hada, and H. Nakatsuji, J. Chem. Phys. **101**, 1029 (1994) and references cited therein.

[27] H. Nakatsuji, M. Ehara, and T. Momose, J. Chem. Phys. **100**, 5821 (1994), and references cited therein.

[28] H. Nakatsuji, J. Ushio, and T. Yonezawa, Can. J. Chem. **63**, 1857 (1985); Y. Mizukami and H. Nakatsuji, J. Chem. Phys. **92**, 6084 (1994); H. Nakatsuji and M. Ehara, Chem. Phys. Lett. **172**, 261 (1990).

[29] H. Nakatsuji and M. Hada, J. Am. Chem. Soc. **107**, 8264 (1985); **109**, 1902 (1987); H. Nakatsuji, Y. Matsuzaki, and T. Yonezawa, J. Chem. Phys. **88**, 5759 (1984); H. Nakatsuji and H. Nakai, Chem. Phys. Lett. **174**, 283 (1990); J. Chem. Phys. **98**, 2423 (1993); H. Nakatsuji, R. Kuwano, H. Morita, and H. Nakai, J. Mol. Catal. **82**, 211 (1993).

[30] J. Geertsen, M. Rittby, and R. J. Bartlett, Chem. Phys. Lett. **164**, 57 (1989); D. C. Comeau and R. J. Bartlett, *ibid.* **207**, 414 (1993); J. F. Stanton and R. J. Bartlett, J. Chem. Phys. **98**, 7029 (1993).

[31] D. Mukherjee and P. K. Mukherjee, Chem. Phys. **39**, 325 (1979).

[32] (a) H. Koch and P. Jørgensen, J. Chem. Phys. **93**, 3333 (1990); (b) H. Koch, H. J. A. Jensen, P. Jørgensen, and T. Helgaker, *ibid.* **93**, 3345 (1990); (c) H. Koch, R. Kobayashi, A. S. de Merás, and P. Jørgensen, *ibid.* **100**, 4393 (1994).

[33] Compare Eq. (7) with Eq. (1) of Ref. 31(b).

[34] S. Huzinaga, J. Andzelm, M. Klobukowski, E. Radzio-Andzelm, Y. Sakai, and H. Tatewaki, *Gaussian Basis Sets for Molecular Calculations* (Elsevier, Amsterdam, 1984).

[35] P. J. Hay and W. R. Wadt, J. Chem. Phys. **82**, 299 (1985).

[36] M. Dupuis, J. D. Watts, H. O. Viller, and G. J. B. Hurst, program system HONDO7, Program Library No. 544, Computer Center of the Institute for Molecular Science, 1989.

[37] (a) H. Nakatsuji, Y. Matsuzaki, and T. Yonezawa, J. Chem. Phys. **88**, 5759 (1988); (b) C. A. Masmanidis, H. H. Jaffe, and R. L. Ellis, J. Phys. Chem. **79**, 2052 (1975); (c) S. Kato, R. L. Jaffe, A. Komornicki, and K. Morokuma, J. Chem. Phys. **78**, 4567 (1983).

[38] C. J. Ballhausen and H. B. Gray, *Molecular Orbital Theory* (Benjamin, New York, 1964).

[39] The $3\,^1A_1$ state is calculated in a very high energy region. In the SE-CI calculation with the active space of 12 highest occupied MOs and five lowest unoccupied MOs the $8\,^1T_2$ state is calculated at 8.78 eV, while the $3\,^1A_1$ state is calculated at 16.57 eV. Furthermore, a test calculation with the active space *I* indicates that the valence excited states with the A_1 symmetry is located at 9.87 eV. We did not include this state in the present results because (1) Rydberg states exist from 7.4 eV and (2) this state will have small effect on the other states after including the spin–orbit interactions.

[40] C. E. Moore, *Atomic Energy Levels* (Nat. Bur. Stand. U.S. Government Printing Office, Washington, D.C., 1971), Vols. 1–3.

[41] J. S. Griffith, *The Theory of Transition Metal Ions* (Cambridge University, Cambridge, 1961).

[42] B. D. Bird and P. Day, J. Chem. Phys. **49**, 392 (1968).